ELSEVIER

Journal of Structural Geology 26 (2004) 1499–1510

JOURNAL OF STRUCTURAL GEOLOGY

www.elsevier.com/locate/jsg

Anisotropy quantification: the application of fractal geometry methods on tectonic fracture patterns of a Hercynian fault zone in NW Sardinia

Sabine Volland[a], Jörn H. Kruhl[b,*]

[a]*Chair of General, Applied and Engineering Geology, Faculty of Civil and Geodetic Engineering, Technische Universität, D-80290 München, Germany*
[b]*Tectonics and Material Fabrics Section, Faculty of Civil and Geodetic Engineering, Technische Universität, D-80290 München, Germany*

Received 17 December 2002; received in revised form 15 August 2003; accepted 22 October 2003

Available online 11 March 2004

Abstract

Three different fractal geometry methods for pattern analysis are applied on a quartz-filled late-Hercynian fracture zone in NW Sardinia. Fragment–size distribution analysis and the box-counting method offer the possibility to (i) detect self-similarity of patterns and, therefore, argue for a specific pattern forming process, and (ii) allow the quantification of the patterns and their comparison with other patterns from similar natural and artificial environments. The failure of these methods in analyzing pattern anisotropies can be overcome by the Cantor-dust method, direction-related and based on the analysis of 1-D distribution of material in relation to its 2-D orientation. With the aid of fractal-dimension orientation diagrams (DOD), a specific parameter, the azimuthal anisotropy of fractal dimension (AAD), can be determined. It quantifies the pattern anisotropy and, consequently, provides the basis for analyzing the pattern-forming processes. In addition, the Cantor-dust method shows the existence of two different pattern-forming processes.

Keywords: Fractal geometry; Fractures; Fracture patterns; Pattern anisotropy; Box-counting method; Cantor-dust method; Fractal-dimension orientation diagram; Azimuthal anisotropy of fractal dimension

1. Introduction

Methods of fractal geometry are increasingly used to analyze a large variety of geological patterns, most prominent amongst them fracture patterns on largely different scales. Such methods offer the opportunity, first, to find a quantitative measure of the pattern and, second, to receive information on pattern-forming processes, their interference, or about the anisotropy and the local variation of a pattern. In the past, fracture zones have been investigated with respect to grain-size reduction (Sammis et al., 1986, 1987), particle distributions, based on experiments (Marone and Scholz, 1989), and fracture densities and patterns, mainly based on the box-counting method (e.g. Turcotte, 1986, 1992; Hirata, 1989) or the Cantor-dust method (Velde et al., 1990). It has become clear that different methods show different sensitivities and advantages in relation to the same pattern (Gillespie et al., 1993; Kruhl and Nega, 1996) and that different types of patterns require different analysis methods that partly still need to be developed. In general, the validity of a variety of existing methods has to be tested in relation to different types of patterns. Moreover, there is still a need for more basic knowledge about the different types of fracture patterns and about their relationship to the underlying processes. The present study illustrates the validity of some common methods of fractal geometry to analyze a fracture zone and the fracture-forming processes. In detail, the anisotropy of the fracture pattern is quantified and the size distributions of the fragments are used to unravel a multi-fold fracturing process.

2. The geology of the fracture zone

The analyzed fracture zone discordantly transects the main foliation of the Hercynian basement in the north-western spur of Sardinia (Fig. 1) and is accompanied by numerous small-scale sub-parallel fractures. The zone is sub-vertical and trends NNW–SSE. It is exposed over a

* Corresponding author. Tel.: +49-89-289-25870; fax: +49-89-289-25852.

E-mail addresses: joern.kruhl@geo.tum.de (J.H. Kruhl), sabine.volland@geo.tum.de (S. Volland).

0191-8141/$ - see front matter © 2004 Elsevier Ltd. All rights reserved.
doi:10.1016/j.jsg.2003.10.005

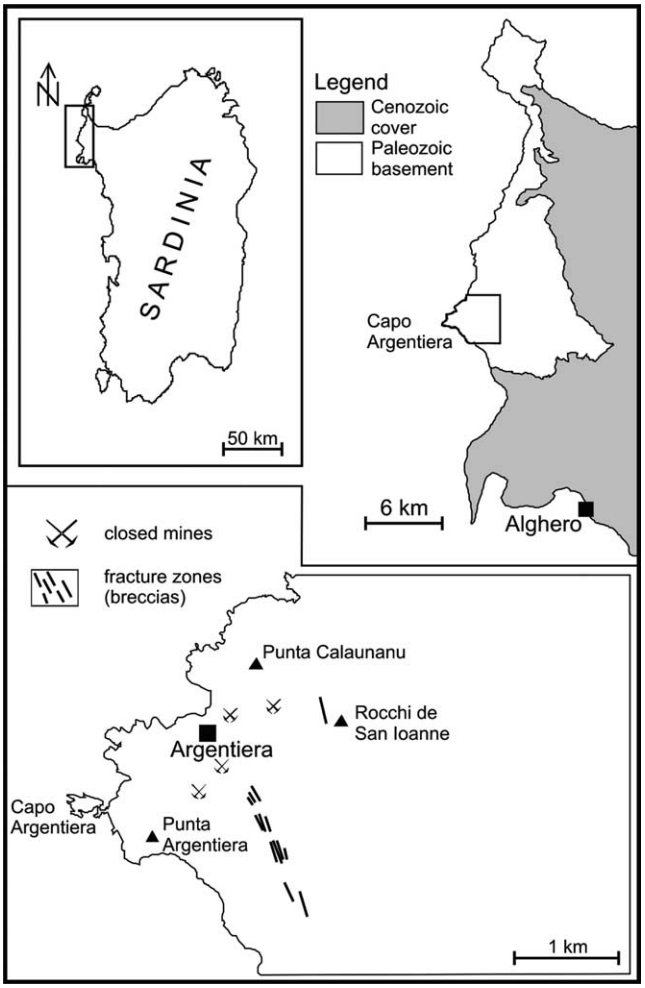

Fig. 1. Study area around Argentiera, with fracture zones and closed mines, within the Paleozoic basement of northwestern Sardinia.

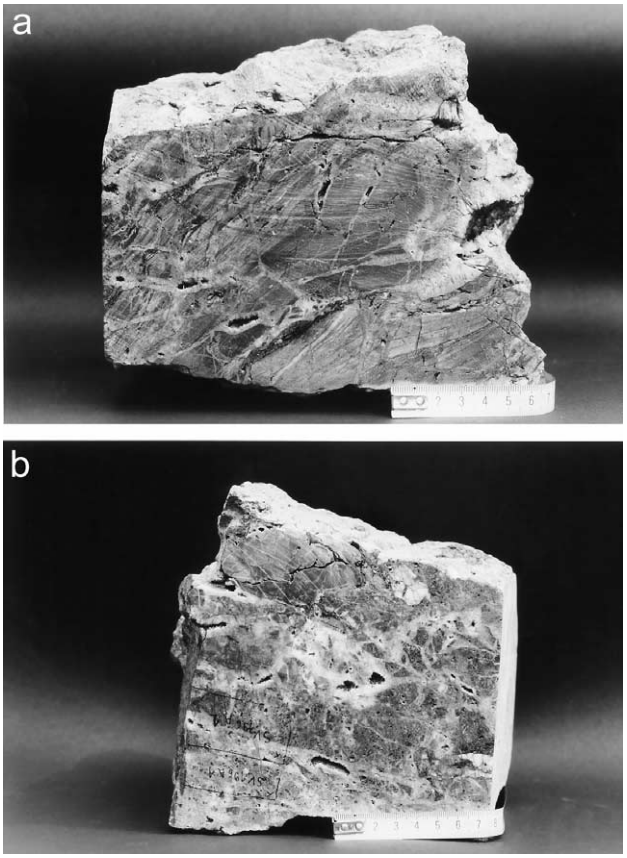

Fig. 2. Studied sample of a fracture zone with two parallel sections a and b. The quartz-filled fractures (white) crosscut the greenschist facies psammopelitic wall rocks (light grey). Locally, millimetre-to-centimetre large cavities, partly filled with euhedral quartz, are developed. Note that the view direction for the two sections is opposite.

length of 100–130 m and a width of ca. 30 m (Volland, 1999) and most probably results from late-Hercynian strike-slip movements. It is part of a larger-scale system of fault zones in western Sardinia that is related to a rich polyphase ore mineralization (Zuffardi, 1989; Pirri, 1996), the basis of intensive mining in prehistoric times (Ottelli, 1996). Several fluid pulses mobilized syn-sedimentary sulphide ores that impregnated the surroundings of the fault zones.

The wall rocks of the fracture zone are highly brecciated. Centimetre to micrometer sized rock fragments are enclosed by a light-grey, whitish and partly light pink quartz matrix (Fig. 2). Cavities with euhedral quartz crystals radially grown around the rock fragments indicate open space during fracture formation. Fluid infiltration into the fracture zone occurred during several pulses as indicated by growth zonation of the euhedral quartz crystals (Fig. 3). The smaller fragments commonly develop rounded edges. The larger fragments are themselves marginally fractured or totally transected by quartz-filled fractures and mostly develop angular shapes with often curved faces, possibly indicating dissolution fluid penetration. In addition, on specific sections the fragments show a weak asymmetric shape orientation (Fig. 4a in comparison with Fig. 4b). The locally round edges of the fragments and the incomplete fractures, penetrating the larger fragments marginally, point to a high hydrostatic pressure, exceeding the lithostatic pressure and to a low differential stress of $<$ca. 20 MPa as

Fig. 3. Photomicrograph of a quartz crystal from the fracture filling. Growth zoning is marked by planes of fluid inclusions parallel to the rhombohedral faces of the quartz crystal against an open cavity. Long side of photomicrograph = 1.02 mm. Crossed polarizers.

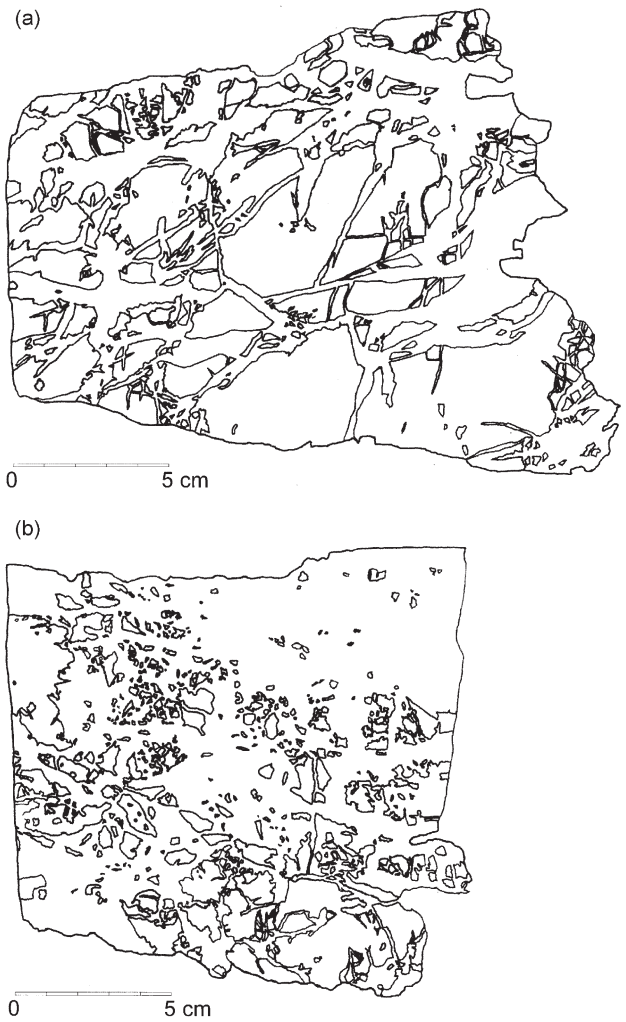

Fig. 4. Sketches of the sample sections a and b.

shown by Simpson (1998) for the metasediments of NW Sardinia.

3. The measurements

Two parallel sections, 20 cm apart, from a breccia in the fracture zone have been analyzed. Each section has an area of 10–13 × 13–18 cm. With the aid of an ink drawing pen with 0.25 mm line thickness the outlines of the fragments have been manually sketched on a transparency, laid over the section, and subsequently digitized. Because the outline of the fragment coincides with the outer rim of the drawing pen line it can be precisely traced and an artificial enlargement of the fragments by the thickness of the line can be excluded. However, the accuracy of the sketch is limited by the thickness of the line. Consequently, particles smaller than ca. 1 mm^2 have not been measured. All measurements have been made on the basis of line drawings of 1.13–1.16 times the original size. The results have been normalized to the original size of the sections.

4. Analysis methods

Typically, the three-dimensional fracture zones are analyzed in two dimensions and the results are transferred to three dimensions, if necessary. In the present study we apply and compare three methods on a breccia sample from a fracture zone: (1) fragment–size frequency histograms, together with the presentation of cumulative curves in log–log diagrams, which represent the application of fractal geometry on data sets, (2) the box-counting method that provides information about the general fracture pattern of the fracture zone, and (3) the Cantor-dust method that is sensitive to the shape anisotropy of fragments.

4.1. Fragment–size frequency distributions

In sedimentology, petrology and other fields of geoscience, e.g. grain-size distributions have traditionally been presented as cumulative curves (e.g. Pettijohn, 1975) and have proven their usefulness as a simple and powerful analytical tool. In applications of fractal geometry this tool has been taken, modified and extended. In relation to size distributions of tectonic fragments, such as the ones presented in this study, the data sets may show fractal patterns and provide information about the fracturing process.

The areas of the fragments in the two studied sections *A* and *B* have been measured with the aid of a millimetre-grid, lain over each of the fragments, by counting all millimetre boxes covered by the area of the fragment. The boxes along the fragment margins covered only partly by the fragment are included in the measurements. This causes a slightly increased fragment size but the increase is negligible compared with the true fragment size. The fragment areas, grouped in 10 mm^2 steps, are presented as frequency distribution diagrams and as cumulative frequencies in a double-logarithmic plot (Fig. 5A and B). The frequency distribution diagrams are in agreement with the visual impression of the two sample sections (A and B) and show for section A the generally larger fragment sizes. The two log–log plots with their approximately linear correlation prove the power-law distribution of the fragment sizes if the largest fragments are excluded, which do not occur in a statistically suitable number. On the other hand, the smallest, i.e. 1 mm^2 fragments strongly deviate from the linear correlation. This is caused by the fact that some of the very small fragments may be missed during the preparation of the line drawing of the natural fracture pattern, as is generally typical of the size distribution analysis of natural objects in geoscience. The slopes of the regression lines are determined as −0.7948 (Fig. 5A) and −0.9533 (Fig. 5B). The standard deviations 0.0053 and 0.0038 suggest that both size distributions can be regarded as different. The smaller slope of section A, compared with B, indicates the higher number of large fragments in relation to the smaller fragments, as seen in the line drawings of the sections

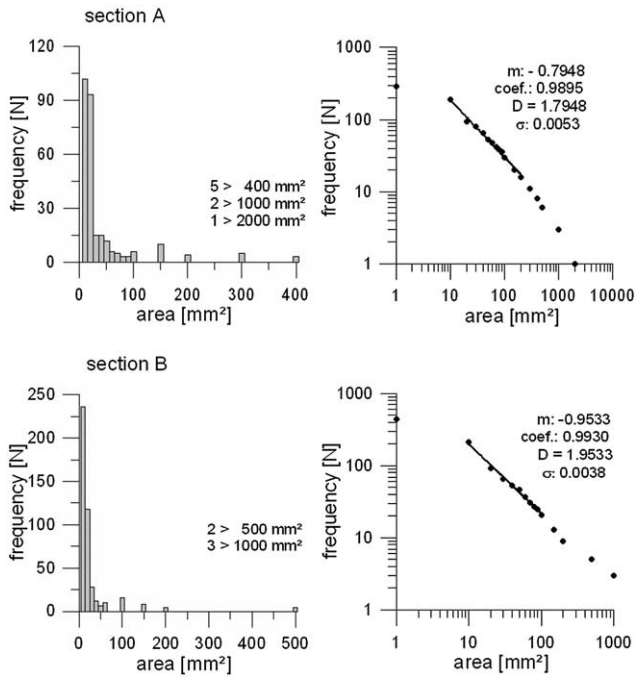

Fig. 5. Frequency distribution (left) and double-logarithmic plot (right) of fragment sizes measured on sample sections A and B. The numbers of fragments larger than 400–1000 mm^2 are indicated; m = slope of the regression line; coef = correlation coefficient, D = fractal dimension, σ = standard deviation.

(Fig. 4). Nevertheless, both frequency distributions follow a power law, the implications of which will be discussed further below.

4.2. Box-counting method

The box-counting method (Feder, 1988; Kaye, 1989; Peitgen et al., 1992, 1998; and many others) is a widely used method of fractal geometry due to its simplicity and capability of being easily automated. A grid of square boxes of side length s is superimposed on the structure, which is on a line pattern. The numbers of boxes that are not empty are counted. This procedure is repeated for as large a range of s-values as possible. Finally, the number $N(s)$ of the transected squares are plotted versus the reciprocal size ($1/s$) of the squares in a double-logarithmic diagram. These data points exhibit a linear correlation if the investigated pattern is a fractal. The slope m of this linear correlation represents the fractal 'box-counting' dimension D_B. In a plane D can never exceed two (Hirata, 1989; Peitgen et al., 1992, 1998).

The box-counting method is suitable for giving a quantitative measure of the geometry, the length and the spatial distribution of fracture and fault patterns in any order of magnification. Above all, it can be applied to patterns with specific scaling properties (Peitgen et al., 1992, 1998) like the studied breccia. However, in the literature different types of box-counting methods are applied and have been proven to be of different significance in evaluating self-similarity and characterizing fracture and fault patterns. They partly have failed to confirm the fractal geometry of fracture patterns (Gillespie et al., 1993). The applied measurement procedure was as follows.

A grid with equal-sized boxes of side length $s = 1/5$, 1/10, 1/20, 1/25, 1/40 and 1/50 of the side length of the initial box was superposed on the two sample section sketches (Fig. 4a and b) as shown in Fig. 6. Then the number of boxes of specific side length, transected by the quartz matrix, was counted and plotted versus $1/s$ in a double-logarithmic diagram (Fig. 7A and B). The relationship between log N and log $1/s$ is strictly linear over about one order of magnitude and proves the self-similarity of the quartz-vein pattern. The slope m of the linear relationship represents the fractal box-counting dimension D_B. The deviation of the data point with the highest $1/s$-value from the regression line is most probably due to the fact that some of the very small fragments may be missed during the preparation of the line drawing of the natural fracture pattern.

Despite the qualitatively different appearance of the fracture patterns of sections A and B (Fig. 4), with large fragments in section A and a high number of small fragments in section B, the fractal box-counting dimensions D_B (1.8551 for section A and 1.8873 for section B; Fig. 7) are similar, giving an average value of ca. 1.87.

4.3. The Cantor-dust method

The sample sections show that at least in section A the shapes of the fragments are generally anisotropic, i.e. their axial ratios are clearly different from one and their long axes show a preferred orientation (Fig. 4a). This type of anisotropy cannot be investigated by the 2-D box-counting method but requires a method working in 1-D. One such method of anisotropy quantification is based on the Cantor set (Peitgen et al., 1992, 1998). The classical Cantor set can be graphically constructed by the subsequent removal of

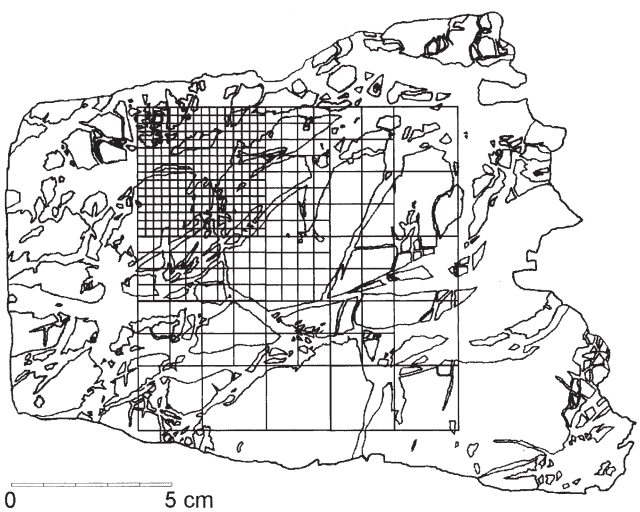

Fig. 6. Sketch of sample section A and part of the box-counting grid with increasingly smaller boxes for each of the measurement steps.

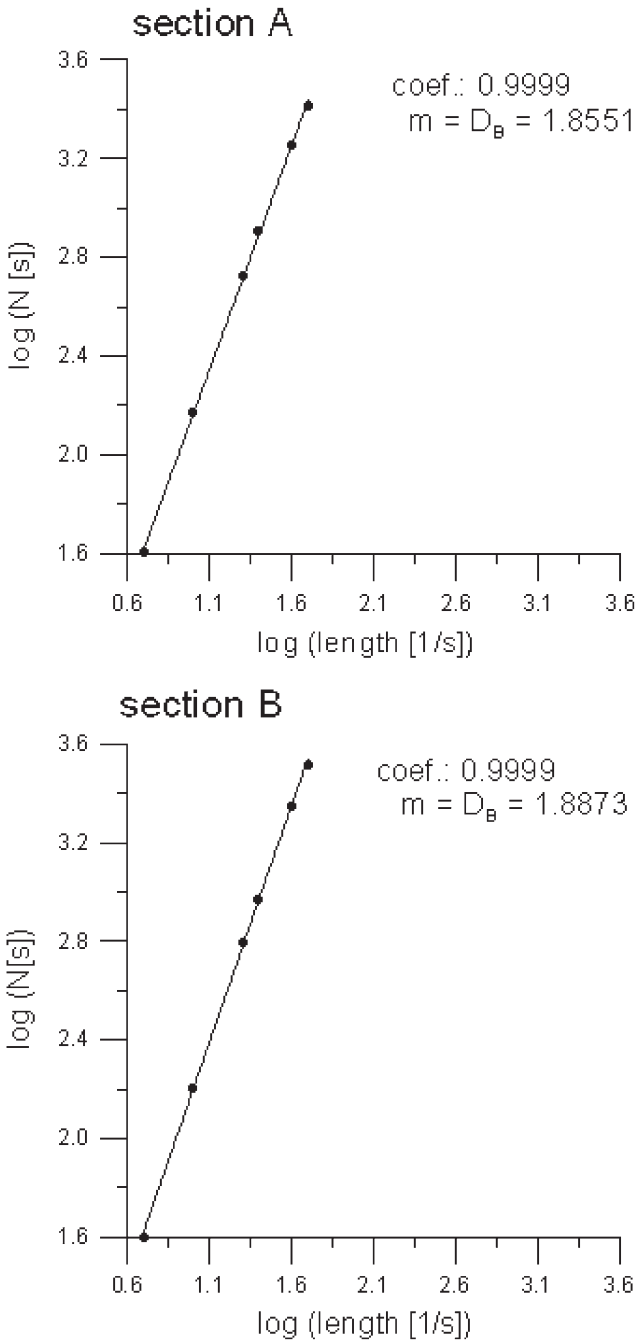

Fig. 7. Representation of the self-similarity of the quartz-vein patterns from the two sample sections A and B as shown in Fig. 4. In a double-logarithmic plot (Richardson plot) the number N of the boxes with side length s, transected by the quartz matrix, is plotted versus $1/s$. The box-counting dimension D_B is equal the slope m of the linear regression line; coef = the regression coefficient.

sections from an initial line of length one (Fig. 8). If the removal procedure is repeated infinite times it leads to an infinite number of points, the so-called 'Cantor dust' (Mandelbrot, 1982). The sequence of Cantor sets produced this way represents a self-similar pattern. Since the Cantor dust is a set of an infinite number of points arranged on a line, but of a volume less than the line, it has a fractal

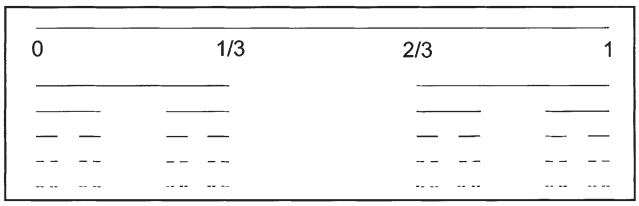

Fig. 8. Construction scheme of a Cantor set. An initial line is divided in several intervals, a certain number of which is removed—one of three in this example. This procedure is repeated infinite times (in this example only four repetitions are shown), leading to an infinite number of points that form a Cantor set, called 'Cantor dust'.

dimension D, with $0 < D < 1$. Methods based on the Cantor dust offer opportunities to study the distribution of material in one dimension and have been applied in geology to the thickness distribution of veins, fractures and faults (Nagahama, 1991; Kruhl, 1994), spacing of veins (Manning, 1994; Simpson, 2000) and fractures (Velde et al., 1990, 1991; Blenkinsop, 1993; Barton, 1995), or the distribution of geological events (Smalley et al., 1987; Dubois and Cheminée, 1988).

Two different types of 1-D analysis are generally applied, (i) the *spacing population technique* (Harris et al., 1991) and (ii) the *interval counting technique*, the 1-D equivalent of the 2-D box-counting method (Velde et al., 1990, 1991). The first one is seen as the more suitable since (i) it infers the fractal dimension directly from a point arrangement along lines through the fracture pattern, and not on the basis of another—the box-counting—procedure like the *interval counting technique*, and (ii) it can discriminate different types of planar geological structures. However, the *spacing population technique* is sensitive to truncation effects (see discussion by Gillespie et al., 1993).

On the basis of the *spacing population technique* we investigated the anisotropy of the quartz vein patterns or the shape anisotropy and alignment of the fragments, respectively. Parallel lines, spaced 5 mm apart, were superposed on the line drawing of the quartz-vein patterns of both sample sections and oriented in 18 different directions of 10° difference each (Fig. 9). Subsequently, the lengths of the line segments in the fragments (in Fig. 9 shown in bold) were measured with an accuracy of 0.1 mm. Their cumulative frequency distribution is presented in a double-logarithmic plot and illustrated for 60° and 140° directions in both sections (Fig. 10). The data points can be divided into two intervals with different linear regressions and, consequently, two different slopes of the regression lines. This holds for the diagrams of all the other directions (Volland, 1999). The subdivision is based on the clear difference of the slopes m_1 and m_2. Despite the local scattering of the data points, all correlation coefficients are near or above 0.99 and all standard deviations are (mostly far) below 0.01. For all line orientations the switch from one regression line to the other occurs between segment lengths of 6 and 7 mm for section A and between 3 and 4 mm for section B. This, again, holds for the diagrams of all the other

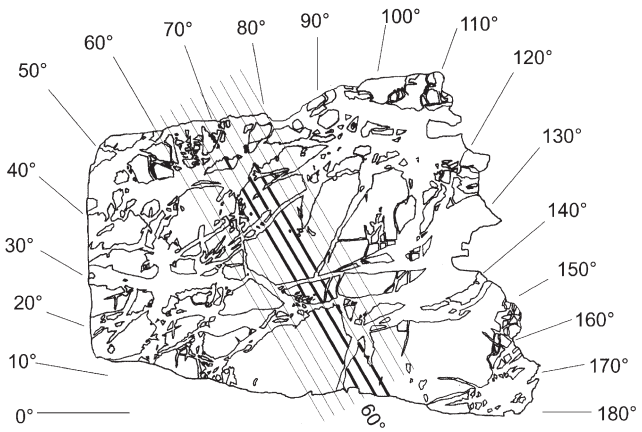

Fig. 9. Measurement procedure for the construction of direction-dependent fragment segments, which form the data basis for the determination of direction-dependent fractal dimensions, presented in Fig. 10. Equal-spaced parallel lines with variable orientation, in this example 60° deviating from the horizontal, define segments of certain lengths. For three lines the segments are shown in bold.

directions, not shown here. Larger segments of lower frequency (below 10–20) have been excluded because their small number implies large fluctuations and, therefore, does not allow an 'objective' computation in the large-size domain. The deviation of the data points including the shortest segments (below 1.2 mm for section A and 1 mm for section B), from the regression line to lower frequencies is most probably due to the fact that such small segments are more easily missed during the measuring procedure than larger segments. The high correlation coefficients, the low standard deviations and the clear subdivision into two slopes at the same segment length for each of the two sections support the view of a general linear regression over about 0.5–1 decade of scale. Such small intervals of linear regression are typical for natural geological structures and do not argue against the validity of such correlations. The slopes of the regression lines define the fractal dimension D of the data set of fragment segments. Such different fractal dimensions are common in various types of natural patterns or natural-pattern-based data sets (Kaye, 1989). The occurrence of different fractal dimensions points to a more complex structure of the pattern or data set and has been

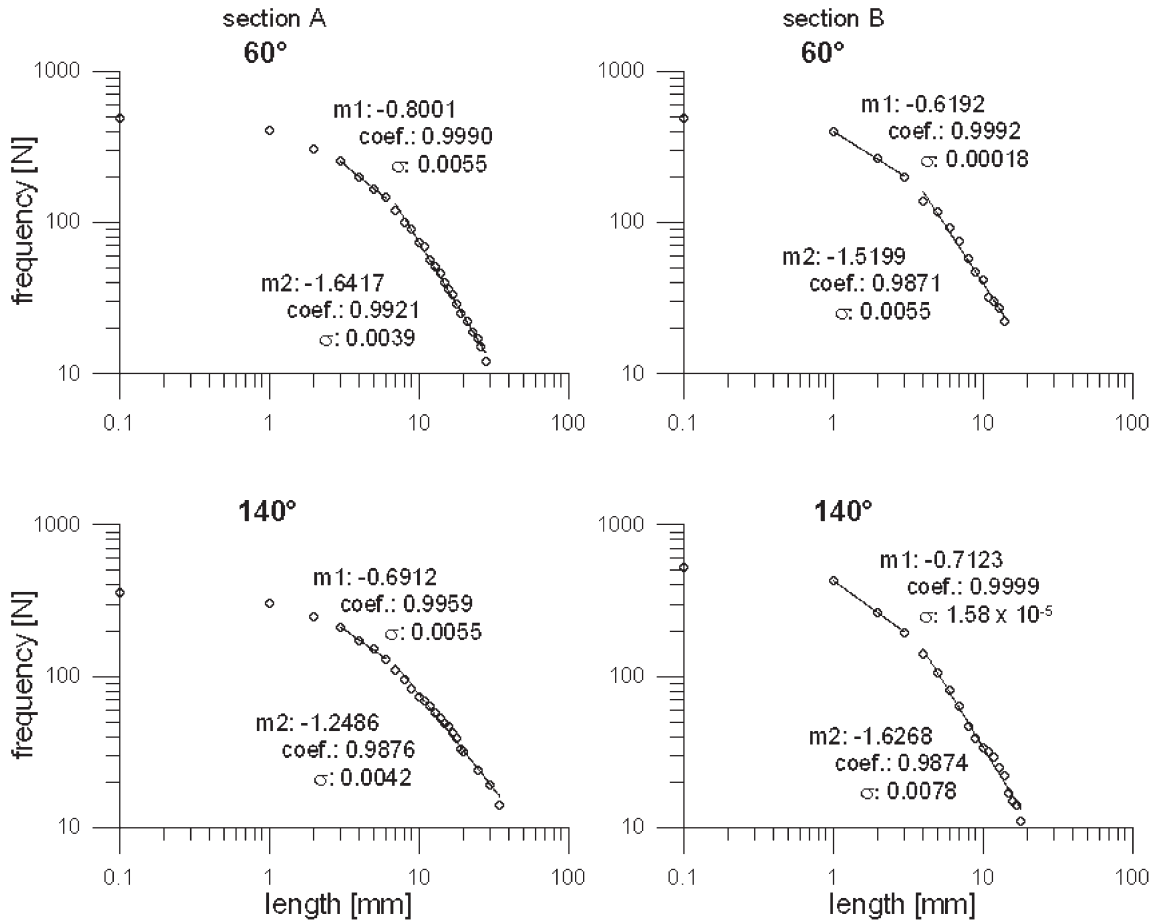

Fig. 10. Double-logarithmic plot of segments formed by two lines of different orientation (60° and 140°), as shown in Fig. 8, each for sections A and B. The data points of the four diagrams can be divided in two groups with different linear regression and, consequently, two different slopes (m_1 and m_2). The lengths of the correlation lines span those data points that have been included in the logarithmic correlation (closed circles). The correlation coefficients (coef) and the standard deviations (σ) are indicated for each regression line.

interpreted as an indication of different subsequent processes (Kaye, 1989; Kruhl and Nega, 1996).

In order to gain information about the anisotropy of the quartz-vein pattern, the fractal dimensions (slopes of the regression lines) have been plotted in relation to the line orientation. These *fractal-dimension orientation diagrams* (DOD; Fig. 11) are similar to those direction-versus-slope diagrams shown by Velde et al. (1991), based on the *spacing population technique*. A complete isotropy of the pattern would be reflected by the same fractal dimension for all directions. In that case the data points would be oriented on a half-circle around the centre of the diagram. However, all four diagrams show a clear deviation from such a configuration. The data points approach an elliptical distribution (Fig. 11), more closely in section A and less in section B. The orientations of the long and short ellipse axes *a*and *b* represent the orientations of maximum and minimum fractal dimension. The axial ratio is named *azimuthal anisotropy of fractal dimension* (AAD).

5. Discussion

Three fractal-geometry-related methods have been applied to a quartz-filled late-Hercynian fracture zone in NW Sardinia. They provide different types of information on the structure and development of this zone and argue for the usefulness of fractal geometry for analyzing brittle deformation structures.

1. Cumulative fragment–size frequency curves give a first hint that the geometry of fragmentation is power-law related, as is typical for fragmentation-produced particle-size distributions (Turcotte, 1986; Sammis et al., 1986, 1987; Kaye, 1989; Nagahama, 1993). Moreover, the generally different particle-size distributions of the two sections are quantified. The fractal dimensions of the distributions, i.e. the absolute values of the slopes of the regression lines, differ from ca. 1.7948 for section A to 1.9533 for section B and reflect the different relative quantity of the particles of different size. The value of section A is nearly equivalent to those values found by Marone and Scholz (1989) in their shear experiments on quartz–sand layers. In these experiments, scale-independent particle-size distributions with a 2-D related fractal dimension D of ca. 1.8 were found, under a hydrostatic pressure of 100 MPa and increasing with increasing strain rate. The value of section B differs clearly, compared with the comparatively low standard deviations of 0.0053 and 0.0038. This possibly points to an anisotropy of the fracture pattern perpendicular to the plane of the sections. However, this can be only evaluated with a higher number of parallel sections.
2. Despite certain limitations (Gillespie et al., 1993), the box-counting method can be regarded as a powerful and easily applicable method to get basic information about a fracture pattern. In our case study, for both sections the self-similarity of the quartz-vein pattern over about one order of magnitude is shown, with a fractal box-counting dimension D_B of about 1.87. This is slightly higher than most of the previously published values (Hirata, 1989; Wanatabe and Takahashi, 1995). Hirata (1989) published D_B values of up to 1.7 for fracture patterns from the centimetre- to the 100-kilometre-scale in different regions of Japan, with the highest values for highly fractured regions. Bour and Davy (1997) found D_B values of 1.9 for large-scale and intensive fracture networks. In general, the fractal dimension of a 2-D pattern increases when the pattern increasingly 'fills' the plane (Mandelbrot, 1982). Therefore, the D_B of about 1.87 indicates the high complexity of the pattern, i.e. the high degree of fragmentation of the studied fracture zone. On the other hand, the measured pattern does not consist of thin lines but of more or less wide stripes or irregular regions and, consequently, it is more 'plane-filling'. That may well serve as an additional reason for the relatively high D_B value.
3. A specific type of the Cantor-dust method, the *spacing population technique*, applied on the segment lengths of the fragments reveals distinct regimes of different fractal dimensions of the data sets and the anisotropy of the fragment shapes and orientations. Two different linear correlations, i.e. fractal dimensions, exist for smaller and larger fragments (Fig. 10). The switch from one to the other linear correlation is independent of the orientation of the measurement lines but occurs at different values for the two sections A and B. In general, such different fractal dimensions are interpreted as reflecting different combined or independent processes or changes of the internal structure of material, which lead to different shapes on different scales. For example, the outlines of mineral grains may lead to a certain fractal dimension and their arrangement in larger arrays may result in another fractal dimension on a larger scale, named *textural* and *structural* fractal dimension (Orford and Whalley, 1983; Kaye, 1989). On a small scale, fractures in rocks may be related to the shape of the crystals, whereas on a larger scale the arrangement of the crystals may be the governing factor. Two different fractal dimensions of grain boundary patterns have been interpreted as the result of two subsequent events of grain boundary migration, i.e. of two different deformation processes (Kruhl and Nega, 1996).

In the present study we interpret the two different fractal dimensions, related to the fragment sizes, as the result of two subsequent tectonic processes. The first one is related to shearing on a regional scale, which fractured the rocks and led to the shape and orientation anisotropy of the fragments. This event is related to the regional late-Hercynian

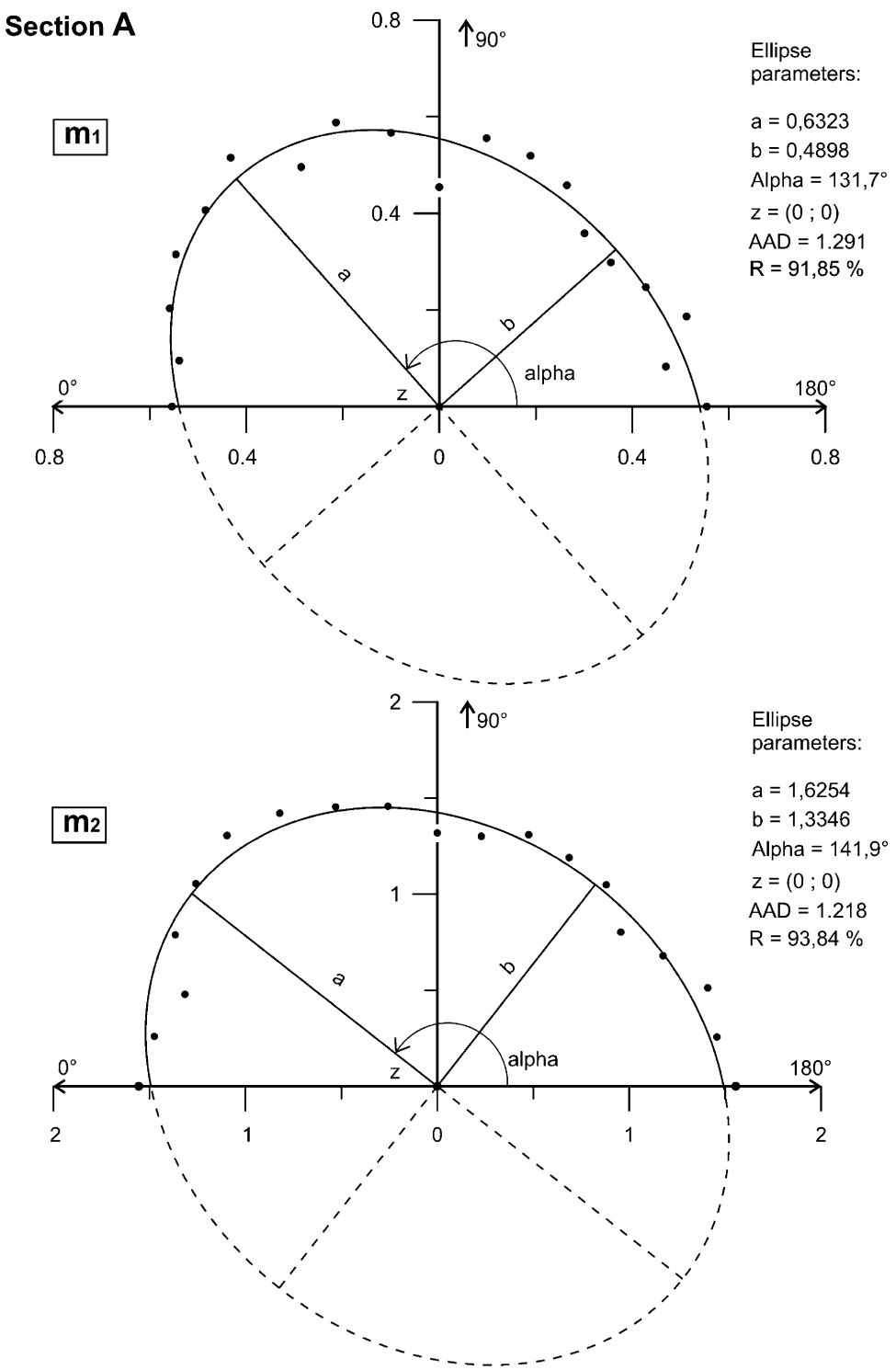

Fig. 11. *Fractal-dimension orientation diagrams* (DOD) of both sections A and B: In a dimensionless circular coordinate system, slopes m_1 and m_2 of the regression lines, as exemplified in Fig. 9, are presented for 18 different directions in 10° steps from 0° to 180°. The 0°/180° line is shown in Fig. 9 and is identical with the orientation of the scale bar in Fig. 4a and b. The slope values are plotted as distances from the centre (z) of the diagram towards the outside. Note that the two diagrams of section B are reflected at the vertical (the 90° line) to get the same view direction as the section A diagrams and facilitate comparison. For each of the four diagrams the best-fit regression ellipses are drawn on the basis of a matlab subroutine after Gander et al. (1994), together with their long and short axes, a and b, and the inclination alpha of a versus the 0/180° line. R is the correlation coefficient. The ratio of a and b is named the *azimuthal anisotropy of fractal dimension* (AAD).

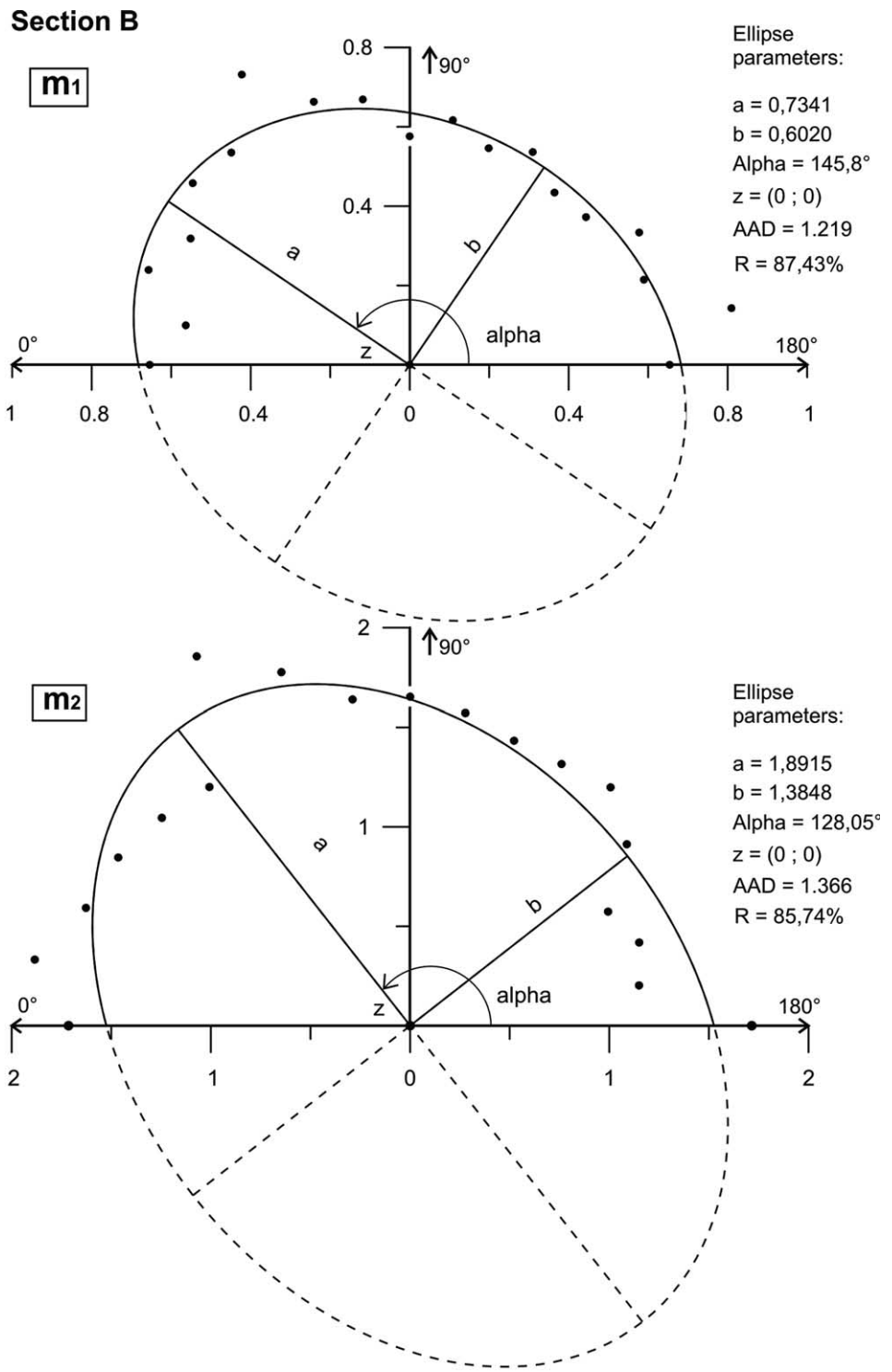

Fig. 11 (*continued*)

deformation of the already cool continental crust in northwestern Sardinia (Carmignani et al., 1979; Francescelli et al., 1990). Adjacent to the study area, numerous fracture zones occur isolated from each other. They possibly represent zones of shear concentration that are related by large-scale fracture systems, as has been suggested for similar situations elsewhere (Bour and Davy, 1997). The relatively high D_B value of ca. 1.87 argues for a position of the studied sample near the local centre of a fracture zone.

The second tectonic process is represented by the dilation of the fracture zone, most probably under fluid overpressure. The opening space was penetrated by fluids and filled by

precipitated quartz during several stages, as indicated by the growth zoning of the undeformed quartz crystals in the quartz veins filling the fracture pattern (Figs. 2 and 3). Quartz-filled en-échelon veins in the wall-rocks of the fracture zone indicate that dilation occurred during shearing. We think that this process led to additional diminution of the existing fragments and to their dismembering to smaller pieces, resulting in a lower number of relatively large fragments. As a possible consequence, a power-law relationship with a higher fractal dimension developed (Fig. 10).

The presentation of the different fractal dimensions in relation to different directions on the measured sections A and B (Fig. 11) is a powerful tool to visualize the 2-D fragment patterns. However, we emphasize that the fractal dimensions and their variation do not directly represent the shapes of the fragments and their orientation anisotropy, even if a general reverse relationship exists. A comparison of Figs. 9 and 11A shows that those directions with relatively short fragment segments are coupled with relatively large fractal dimensions and vice versa. This is due to the fact that a power-law relationship assumed that an increased number of short fragments leads to a larger slope of the regression line in the double-logarithmic length-versus-frequency diagram (Fig. 10) and vice versa. Various inferences can be made from these *fractal-dimension orientation diagrams* (DOD).

First, the different D-values related to different directions, or the deviation of the data points from a circular arrangement, indicate the general anisotropy of the fragment patterns. A smooth D-function of orientation may be expected for natural fracture patterns that are typically highly irregular, even if this does not necessarily hold for specific artificial patterns (see discussions by Harris et al. (1991) and Velde et al. (1991)). The data points roughly show an elliptic arrangement (Fig. 11) that reflects the shearing in 2-D. The best-fit ellipse, i.e. the idealized representation of the data points, can be taken as a measure of the general anisotropy of the fragmentation patterns. It is characterized by the ratio of the long and short principal axes, the ellipticity, which increases with increasing deviation of the ellipse shape from a circle. Consequently, the anisotropy can be represented by one single number, the axial ratio of the ellipse, or the ellipticity (AAD). If the AAD is related in some way to the orientation of the stress field, as has been suggested by Velde et al. (1990) for the orientation variation of D based on the *interval counting technique*, or to a combination of the external stress field with internal forces and the structure of the material, remains an open question and would need intensive, mainly experimental, investigations.

Second, the correlation coefficient (R) is a measure of the scattering of the data points around the best-fit ellipse and, therefore, indicates the direction-related homogeneity of the pattern. In addition, local specific deviations of the data points from the elliptical arrangement indicate specific directions of pattern anisotropy. For example, D in relation to the 90° direction is relatively low in section A/slope m_1, section A/slope m_2 and section B/slope m_1 (Fig. 11), and in relation to 60° and 70° it is relatively high, with the exception of 60° in section A/slope m_1. Because all standard deviations of the fractal dimensions are far below 0.01, at least these larger differences appear to be significant. The nature and meaning of this pattern anisotropy are still uncertain but obviously cannot be correlated straightforward with fracture orientations, as in the simple case of orthogonal tension faults that lead to an orthogonal direction-related distribution of D values (Velde et al., 1990; Fig. 2). If such complex data point distributions in a *fractal dimension orientation diagram* comprise additional useful information on the pattern-forming processes and their interaction with the material is a question of further detailed investigations.

Third, in relation to our case study, the fragment patterns show a clear anisotropy with AAD values ranging from ca. 1.22 to 1.37, with highest D values related to approximately the same direction on both sections and for both linear-regression intervals (with slopes m_1 and m_2), as indicated by the similar ellipse inclination alpha (Fig. 11). If we exclude the AAD value of section B/slope m_2 because of the low elliptical fit, indicated by the low correlation coefficient R, the remaining three AAD values are very similar. The similarity between the AAD values of section A/slope m_1 and slope m_2 can be interpreted to indicate that the fracture zone dilation under fluid overpressure did not change the pattern anisotropy and, therefore, possibly still acted during shearing. The similarity between the AAD values of section A/slope m_1 and section B/slope m_1 indicates the reproducibility of the AAD values on parallel sections, i.e. its validity for the total volume of the fractured rock sample. On one hand, it may be expected that the same fracturing processes acted on the two sections, taken in the same orientation from the same sample separated by a distance of about 20 cm. On the other hand, a clear anisotropy of the fracture pattern is only visible on section A (Fig. 4a compared with Fig. 4b). Obviously, the anisotropy of section B is more difficult to visualize because of the relatively strong inhomogeneity of the pattern and the generally smaller fragment sizes. In this case, the fractal geometry analysis provides information not accessible by pure visualization.

6. Conclusions

Each of the three applied methods represents a tool of its own value that leads to information of different type and quality. In a first step, the particle size analysis may lead to the detection of a power-law relationship of the particle size frequency distribution and, therefore, to a characteristic fractal dimension of the particle sizes, arguing for one specific fragment-forming process. In addition, the fractal

dimension offers the opportunity of quantification and, therefore, comparison with similar processes in another or the same geotectonic environment and, not least, with the results of deformation experiments. The box-counting method leads to a fractal dimension D_B that, in our case study, characterizes the fracture or quartz-vein pattern. It points to the self-similarity of the pattern over about one order of magnitude and provides, by the fractal box-counting dimension D_B, a quantitative measure of the pattern. The advantage of this method is its easy applicability and that it offers the opportunity of a quantitative comparison of different types of fracture patterns. The disadvantage of the box-counting method is the impossibility of analyzing pattern anisotropies, which are a common phenomenon in natural as well as artificial material.

The present study shows that the Cantor-dust method, modified for analyzing the 1-D distribution of material in relation to directions in 2-D, is a powerful tool for the characterization and quantification of pattern anisotropies and inhomogeneities. It provides information about different regimes of fractal dimensions in relation to a distinct pattern and, consequently, about the presence of different subsequent or contemporaneous pattern forming processes. On the basis of *fractal-dimension orientation diagrams* (DOD), the *azimuthal anisotropy of fractal dimension* (AAD) can be determined. This parameter quantifies the pattern anisotropy and, consequently, allows the comparison between the anisotropies of different patterns. It is also expected to form a useful future basis for the analysis of pattern-forming processes and the interactions between such processes and the structured material.

Acknowledgements

We are grateful to Giacomo Oggiano for introducing us to the beauty of the geology of Sardinia, to Erwin Helbig for making available his random generators Shuffle and DIV, written in AWK, and for fruitful discussions on the data analysis and to Francisc Andries for calculating the best-fit ellipses. Cristian Suteanu provided useful comments on a first draft of the manuscript and two anonymous reviewers on the submitted manuscript. We are specifically grateful to Tom Blenkinsop for his helpful and stimulating comments. The study was funded privately by the authors, and by the Chair of General, Applied and Engineering Geology and the Tectonics and Material Fabrics Section, Technische Universität München.

References

Barton, C.C., 1995. Fractal analysis of scaling and spatial clustering of fractures. In: Barton, C.C., La Pointe, P.R. (Eds.), Fractals in the Earth Sciences, Plenum Press, New York, pp. 141–178.

Blenkinsop, T.G., 1993. Fracture spacing distributions in rock. International Symposium on Fractals and Dynamic Systems in Geoscience, Book of Abstracts, Johann Wolfgang Goethe Universität, Frankfurt am Main/Germany, pp. 6–7.

Bour, O., Davy, P., 1997. Connectivity of random fault networks following a power law fault length distribution. Water Resources Research 33, 1567–1583.

Carmignani, L., Franceschelli, M., Pertusati, P.C., Memmi, I., Ricci, C.A., 1979. Evoluzione tettonico-metamorfica del basamento ercinico della Nurra (Sardegna NW). Memorie della Società Geologica Italiana 20, 57–84.

Dubois, J., Cheminée, J.-L., 1988. Application d'une analyse fractale à l'étude des cycles éruptifs du Piton de la Fournaise (La Réunion): modèle d'une poussière de Cantor. C.R. Acad. Sci. Paris 307, 1723–1729. (cited in: Velde et al., 1990. Tectonophysics 179, 345–352).

Feder, J., 1988. Fractals. Plenum Press, New York, 283pp.

Francescelli, M., Pannuti, F., Puxeddu, M., 1990. Texture development and PT time path of psammitic schist from the Hercynian chain of NW Sardinia (Italy). European Journal of Mineralogy 2, 385–398.

Gander, W., Golub, G.H., Strebel, R., 1994. Fitting of Circles and Ellipses—Least Squares Solution. Report 217. Departement Informatik, ETH, Zürich, 57pp.

Gillespie, P.A., Howard, C.B., Walsh, J.J., Watterson, J., 1993. Measurement and characterization of spatial distributions of fractures. Tectonophysics 226, 113–141.

Harris, C., Franssen, R., Loosveld, R., 1991. Fractal analysis of fractures in rocks: the Cantor's Dust method—comment. Tectonophysics 198, 107–111.

Hirata, T., 1989. Fractal dimension of fault systems in Japan: fractal structure in rock fracture geometry at various scales. Pure and Applied Geophysics 131, 157–169.

Kaye, B.H., 1989. A Random Walk Through Fractal Dimensions. VCH Verlagsgesellschaft, Weinheim.

Kruhl, J.H., 1994. The formation of extensional veins: an application of the Cantor-dust model. In: Kruhl, J.H., (Ed.), Fractals and Dynamic Systems in Geoscience, Springer, Berlin/Heidelberg, pp. 95–104.

Kruhl, J.H., Nega, M., 1996. The fractal shape of sutured quartz grain boundaries: application as a geothermometer. Geologische Rundschau 85, 38–43.

Mandelbrot, B.B., 1982. The Fractal Geometry of Nature. Freeman & Co, New York.

Manning, C.E., 1994. Fractal clustering of metamorphic veins. Geology 22, 335–338.

Marone, C., Scholz, C.H., 1989. Particle-size distribution and microstructures within simulated fault gouge. Journal of Structural Geology 11, 799–814.

Nagahama, H., 1991. Fracturing in the solid earth. Science Report Tohoku University, 2nd series 61, pp. 103–126.

Nagahama, H., 1993. Fractal fragment size distribution for brittle rocks. International Journal of Rock Mechanics and Mining Sciences & Geomechanics, Abstracts 30, 469–471.

Orford, J.D., Whalley, W.B., 1983. The use of the fractal dimension to quantify the morphology of irregular-shaped particles. Sedimentology 30, 655–668.

Ottelli, L., 1996. L'Argentiera—Il Giacimento, la Miniera, gli Uomini. Edizione Gallizzi.

Peitgen, H.-O., Jürgens, H., Saupe, D., 1992. Fractals for the Classroom, Part 1. Springer, New York.

Peitgen, H.-O., Jürgens, H., Saupe, D., 1998. Bausteine des Chaos: Fraktale. Rowohlt, Reinbek, 514pp.

Pettijohn, F.J., 1975. Sedimentary Rocks, 3rd ed, Harper & Row, New York, 628pp.

Pirri, I.V., 1996. The Pb–Zn–Ag–Sb deposit of Argentiera (Nurra, NW Sardinia): an example of direct mineralogical inheritance. Neues Jahrbuch Mineralogie Monatshefte 1996, 223–240.

Sammis, C., King, G., Biegel, R., 1987. The kinematics of gouge deformation. Pure and Applied Geophysics 125, 777–812.

Sammis, C.G., Osborne, R.H., Anderson, J.L., Banerdt, M., White, P., 1986. Self-similar cataclasis in the formation of fault gouge. Pure and Applied Geophysics 124, 53–78.

Simpson, G.D.H., 1998. Dehydration-related deformation during regional metamorphism, NW Sardinia, Italy. Journal of Metamorphic Geology 16, 457–472.

Simpson, G.D.H., 2000. Synmetamorphic vein spacing distributions: characterization and origin of a distribution of veins from NW Sardinia, Italy. Journal of Structural Geology 22, 335–348.

Smalley, R.F., Chatelain, L.-L., Turcotte, D.L., Prevot, R., 1987. A fractal approach to the clustering of earthquakes: applications to the seismicity of the New Hebrides. Bulletin of the Seismological Society of America 77, 1368–1381.

Turcotte, D.L., 1986. Fractals and fragmentation. Journal of Geophysical Research 91, 1921–1926.

Turcotte, D.L., 1992. Fractals, chaos, self-organized criticality and tectonics. Terra Nova 4, 4–12.

Velde, B., Dubois, J., Touchard, G., Badri, A., 1990. Fractal analysis of fractures in rocks: the Cantor's Dust method. Tectonophysics 179, 345–352.

Velde, B., Dubois, J., Moore, D., Touchard, G., 1991. Fractal patterns of fractures in granites. Earth & Planetary Science Letters 104, 25–35.

Volland, S., 1999. Geology and fractal geometry of late to post-Variscan fracture systems from the southern Nurra, northwest Sardinia. Diploma thesis, Technische Universität München, 103pp. (in German).

Wanatabe, K., Takahashi, H., 1995. Fractal geometry characterization of geothermal reservoir fracture networks. Journal of Geophysical Research 100, 521–528.

Zuffardi, P., 1989. Italy. In: Mineral Deposits of Europe. Vol. 4/5: Southwest and East Europe, with Iceland. The Institution of Mining and Metallurgy & Mineral Society, London, pp. 221–274.